Stochastic Modeling of Wind Power Production

Patrick Milan[*] Matthias Wächter[†] Joachim Peinke[‡]

ForWind - Center for Wind Energy Research
of the Universities of Oldenburg, Hannover and Bremen
University of Oldenburg, Germany

Abstract

A stochastic model is proposed to reproduce synthetically the power production of a wind energy converter (WEC) from any given wind measurement. The structure of the model aims towards the high-frequency dynamics of the conversion from wind speed to power output. These dynamics appear to be a superposition of an attractive power curve plus some additional fluctuations stemming from wind turbulence. These adversary dynamics can be characterized through respectively a drift and a diffusion matrix. These two matrices can be inserted into a stochastic equation named the Langevin equation, which can generate a time series of power output from a given time series of wind speed. For this paper, the computation is performed and the time series of power output measured and modeled are compared. Various statistical tests are presented. It can be concluded that the stochastic model reproduces quantitatively well various complex statistics observed on measurements. The tests performed involve ten-minute average values, ten-minute standard deviations, as well as the spectrum and increment PDFs. Beyond the standard ten-minute statistics usually considered, the fast gusts measured in high-frequency are also modeled. Its fast and flexible structure could make the stochastic method useful for a realistic modeling of the intermittent power production of WECs.

Keywords: turbulence, gust, power production modeling, high-frequency dynamics, wind speed/power conversion

[*]patrick.milan@forwind.de
[†]matthias.waechter@forwind.de
[‡]joachim.peinke@forwind.de

1 Introduction

The atmospheric wind in which wind energy converters (WECs) operate is a complex process [1]. Turbulent structures are observed on short time scales in high-frequency wind measurements. While these short-time fluctuations should not affect strongly the annual energy production, they generate important alternating loads on the entire structure of every WEC. Thus raises the question of the negative impact of turbulence on downtimes and on the overall lifetime of a WEC. In parallel, such turbulent wind makes any WEC a fluctuating, intermittent source of energy. Wind gusts are transformed into intermittent, rapidly-changing “power gusts”. When measured at high-frequency ($\approx 1Hz$), the power production fed into the electric grid by a single WEC is a complex, intermittent signal.

Wind turbulence cannot be controlled or reduced at will. The site topography and surface roughness have a direct impact on the turbulence intensity, making some sites less *turbulent* than others, mainly offshore sites. Our rising dependence on wind energy calls for a better understanding of such phenomena, as well as reliable models. However, the staggering level of complexity of turbulent effects makes modeling a complex task. On the one hand, simple models typically neglect the high-order statistics that govern gusts. On the other hand, advanced CFD codes demand so much computer resources that they cannot model entire WECs (yet).

In this paper, a stochastic model is proposed as an alternative. The model converts a high-frequency time series of wind speed $u(t)$ into a high-frequency time series of power output $P(t)$, reproducing the conversion process performed by a WEC.

The stochastic theory used allows for a fast model that reproduces quantitatively well the statistics observed on power output measurements. In a first step, the WEC must be characterized appropriately. In a second step, this characterization, in the form of the drift and diffusion matrix $D^{(1)}$ and $D^{(2)}$ is inserted into a stochastic Langevin equation. A synthetic time series of the power output can then be generated by solving the Langevin equation iteratively.

2 Step 1: characterizing the WEC dynamics

2.1 Data requirements

In order to properly reproduce the power production of a WEC, the stochastic model must be parametrized. The necessary parameters can be extracted from a measurement performed beforehand on the WEC of interest. The variables to be measured are the simultaneous time signals of wind speed $u(t)$ and of net power output $P(t)$ of the WEC. The time series should have a sampling frequency in the order of $1Hz$, as displayed in figure 1. The intermittent, gusty nature of the wind is observed on short time scales. This justifies the need for high-frequency measurements that contain detailed information about the fast fluctuations, and that is unavailable with the standard ten-minute averaging technique used for measurement. Modeling such complex statistics is one important goal of the method presented.

In order to represent the dynamics of the WEC accurately, the original measurement should be long enough to span all necessary wind conditions[1]. The wind speed $u(t)$ should be measured at hub height from a met mast, as described by the IEC power curve standard [2]. Additional data requirements and corrections described in the IEC norm may be applied here for optimal results. Only the

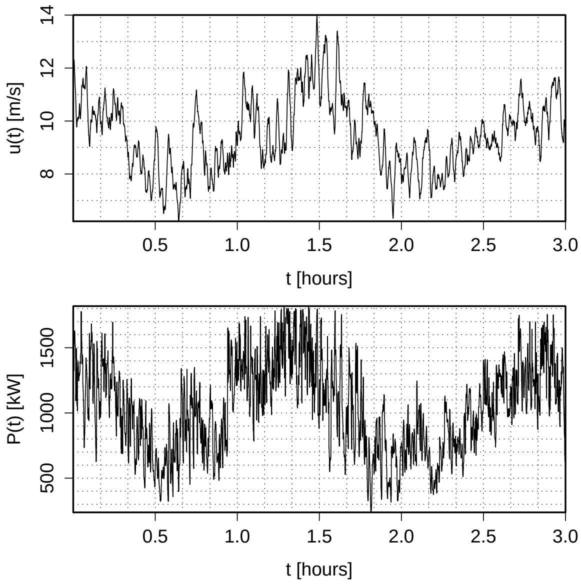

Figure 1: Example of a simultaneous measurement of wind speed $u(t)$ and power output $P(t)$ at frequency $1Hz$. The measurement was performed on an operating multi-MW WEC. It is not the dataset used later on.

sampling frequency of the recorded data *must* be in the order of $1Hz$ instead of the ten-minute averaging applied in the IEC norm. The stochastic model is by nature related to power curve methods, as it aims to convert wind speed into power output. This intrinsic connection makes it a flexible tool which can potentially be applied to any WEC design that displays a clearly defined power curve. It has also been shown to be well applicable together with different wind measurement principles, such as LIDAR [3] or nacelle anemometry measurements.

The data set used contains $900\,000$ datapoints, sampled at $2.5Hz$. This corresponds to a measurement period of approximately 4 days. The wind speed is an actual wind measurement on a met mast at the GROWIAN site in Germany [4, 5]. However, the time series labeled as *measurement time series* of power $P(t)$ used in this paper was obtained from a computer model for a 1.5MW WEC. This other model is a mechanical WEC model named FAST [6]. This model was already accepted to model well the dynamics of a WEC [7]. The reason for using this data is that high-frequency measurements of wind speed and power output are difficult to obtain. Whenever *measurement power* is mentioned in this

[1] How long is enough for a good measurement depends on the wind conditions. A first guess for the necessary duration is in the order of two weeks. Unlike procedures based on ten-minute averaging, the use of high frequency data allows for a faster convergence. It is however expected that longer measurements yields better modeling results.

paper, it should be understood as output of the mechanical model FAST (and input for the stochastic model). An extension to real WEC data is however straightforward whenever measurement data is available, and the result is expected to hold valid.

2.2 Characterizing the dynamics

The stochastic model follows the idea that the power output $P(t)$ can be approximated by a stochastic differential equation named the Langevin equation [8]

$$\frac{d}{dt}P(t) = D^{(1)}(P;u) + \sqrt{D^{(2)}(P;u)} \cdot \Gamma(t)\,, \quad (1)$$

where $D^{(1)}(P;u)$ and $D^{(2)}(P;u)$ are called respectively the drift and diffusion fields, and $\Gamma(t)$ is a Gaussian white noise with mean value $\langle\Gamma(t)\rangle = 0$ and variance $\langle\Gamma^2(t)\rangle = 2$. The stochastic approach consists in solving the Langevin equation, as further described in section 3. Because $\Gamma(t)$ is a set of random numbers, the term $\sqrt{D^{(2)}(P;U)} \cdot \Gamma(t)$ is a stochastic, i.e. random term, and $D^{(1)}(P;u)$ is a deterministic term in the Langevin equation (1). The drift field $D^{(1)}$ represents the dynamical response of the WEC, while the diffusion field $D^{(2)}$ quantifies random turbulent fluctuations together with $\Gamma(t)$, as explained below.
An essential aspect of the method is that the two fields $D^{(1)}$ and $D^{(2)}$ can be estimated directly from measurement data (sampled at the order of $1Hz$), as follows [8, 9]

$$D^{(n)}(P;u) = \frac{1}{n!}\lim_{\tau\to 0}\frac{1}{\tau}$$
$$\langle [P(t+\tau) - P(t)]^n | P(t) = P; u(t) = u\rangle\,, \quad (2)$$

where $\langle | \rangle$ denotes the conditional ensemble average. To this end, the calculation is conditioned over the two-dimensional state space $\{P;u\}$. In a practical sense, the fields $D^{(n)}(P;u)$ are two-dimensional matrices computed in each discrete bin of the two-dimensional space $\{P;u\}$. An illustration of the drift field $D^{(1)}$ is given in figure 2.
The values of the drift field (matrix) $D^{(1)}$ are plotted using arrows in figure 2. The drift is plotted using a blue arrow when positive, i.e. $D^{(1)}(P;u) > 0$, indicating that in these regions the power output $P(t)$ increases (on average). The inverse situation happens for

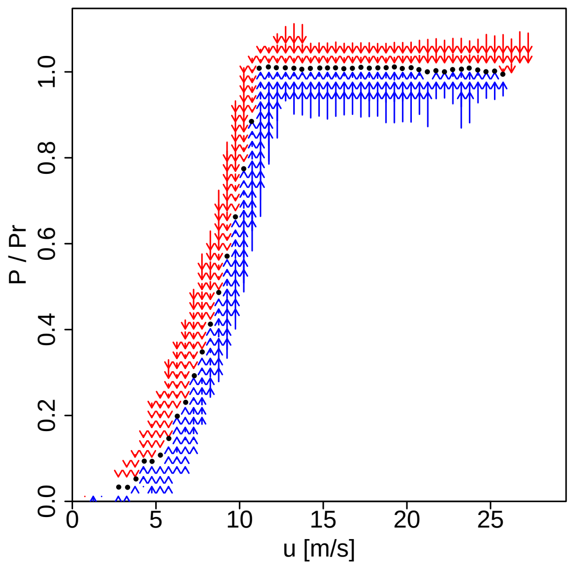

Figure 2: Drift field $D^{(1)}(P;u)$ represented qualitatively using arrows. The local value of drift $D^{(1)}(P;u)$ is represented by the direction and length of each arrow, while the color also indicates the direction of the drift. The black dots represent the stable fixed points where $D^{(1)}(P;u) = 0$, also called the Langevin power curve [7, 10]. The binning chosen here was $0.5m/s$ for u and 50 bins for P. The power is normalized by rated power $P_r = 1500kW$.

the red arrows, where the drift is negative, and the power output decreases. Figure 2 is a map that illustrates how the power production changes for each combination of wind speed and power. The WEC permanently adapts its power production to match with an ever-changing turbulent wind. While the IEC power curve gives the average power corresponding to each wind speed, the Langevin power curve defined as $D^{(1)} = 0$ (black dots in figure 2) represents the stable, attractive dynamics of the WEC[2]. For information, $D^{(1)}$ and $D^{(2)}$ could be estimated only in the bins where measurement data was recorded. The white regions in figure 2 represent these regions where the data never went. This is not a limitation to the model because these regions are not of interest, as the WEC never explores them.
Although the Langevin and IEC power curves

[2] Additionally, $D^{(1)}(P)$ must have a decreasing slope around the stable fixed points. An increasing slope would indicate an unstable fixed point, when only stable fixed points are of interest here.

have a similar shape [11], the Langevin power curve brings additional meaning as it is the dynamical attractor of the WEC in the two-dimensional space $\{P; u\}$. Following this result, the WEC dynamics can be understood in a simple way. The power production is attracted towards the stable fixed points where $D^{(1)}(P; u) = 0$, i.e. the Langevin power curve [7, 10]. Under constant, laminar wind conditions, the WEC would relax towards the Langevin power curve. However, the turbulent wind fluctuations endlessly drive the system away from the stable fixed points. The underlying dynamics of the conversion from wind speed to power output can then be separated into an attractive power curve and the additional turbulent fluctuations driving the system away from the stable power curve. This corresponds exactly to the structure of the stochastic model, where the drift field $D^{(1)}$ represents the attractor displayed in figure 2, and where the diffusion field $D^{(2)}$ quantifies additional, random fluctuations stemming from turbulence[3]. As the WEC dynamics are characterized, the estimated drift and diffusion fields (matrices) can be used in the Langevin equation to simulate the power output $P(t)$ for any given wind speed $u(t)$, as is introduced in section 3.

3 Step 2: modeling the WEC power production

The two matrices $D^{(1)}(P; u)$ and $D^{(2)}(P; u)$ carry the necessary information about the conversion from wind speed $u(t)$ to power output $P(t)$ at high-frequency. It should be noted that the goal of such model is not to reach an exact reproduction of the power time series, but rather to model a time series that has the same statistical properties. The use of a random noise $\Gamma(t)$ makes an absolute, exact reproduction impossible. It is through the proper estimation of the $D^{(n)}$ fields that the correct statistics can be modeled. Their proper estimation is detailed in section 2.2.

The two fields (matrices) must be inserted into the Langevin equation that becomes a model for the power output $P^\star(t)$ of the WEC. For clarity of reading, the power signal originally measured on the WEC will be further labeled $P(t)$, and the power modeled by the Langevin equation $P^\star(t)$. The Langevin equation (1) introduced in section 2.2 is valid for a continuous process. While such process exists only in a mathematical sense, a concrete application requires to adapt the Langevin equation to a form discrete in time, i.e. defined at every discrete time step τ as follows

$$P^\star(t+\tau) = P^\star(t) + \tau \cdot D^{(1)}(P^\star(t); u(t)) + \sqrt{\tau \cdot D^{(2)}(P^\star(t); u(t))} \cdot w(t)\,. \quad (3)$$

According to stochastic calculus, the noise term $\Gamma(t)$ in (1) has to be integrated over the time step τ, leading to the Wiener noise $\sqrt{\tau} \cdot w(t)$, where $w(t)$ is delta-correlated with a variance of 2 (cf. [8], section 3.6). The sampling time τ should be chosen similar to the sampling time of the measurement time series used in section 2.1 to estimate the fields. Additionally, the wind speed $u(t)$ used in the discrete Langevin equation (3) should also be sampled with a similar sampling time. The reason is that the dynamics represented by the two fields is characteristic of the sampling rate of the measurement time series introduced in section 2.1. Using the fields on a very different sampling time makes little sense as they do not characterize the dynamics on this time scale. For consistency, all sampling rates of all signals used should be the same (or at least of similar order). For information, the results displayed in this paper were obtained using $\tau = 0.4s$ (for a sampling frequency $f = 1/\tau = 2.5Hz$).

$\Gamma(t)$ is a Gaussian white noise. This means that it is a series of independent random numbers that are Gaussian distributed. Its mean value must be $\langle\Gamma(t)\rangle = 0$ and its variance $\langle\Gamma^2(t)\rangle = 2$ following [8]. Such random signal can be generated fast and easily from most scientific programming softwares. For example, 10^7 such data points are generated in less than $1s$ on a standard desktop computer by the computing software R [14]. For information, all calculations were performed using R in this project.

Finally, the initial condition $P^\star(t = 0)$ influences only slightly the future evolution as

[3] The authors would like to note that the stochastic theory presented here was successfully applied to other systems such as airfoil lift dynamics [12] or turbulent flows [13]. Numerous complex systems were studied in the same manner in various scientific fields.

$P^{\star}(t)$ will adjust rapidly to the corresponding wind speed $u(t)$[4]. The model can then be run unambiguously to simulate $P^{\star}(t)$.
Because the model must first be constructed from a measurement of $u(t)$ and $P(t)$, the user can always compare the measured signal $P(t)$ with the modeled signal $P^{\star}(t)$. To test the validity of the model, a visual comparison of P and $P^{\star}$ is given in figures 3 and 4.
One can observe in figure 3 that the stochastic model manages to reproduce the measurement signal, at least in a visually satisfying manner. Here, the time series contain so many data points that it is impossible to really distinguish the two signals. However, $P^{\star}(t)$ seemingly spans the same range at $P(t)$, which already guarantees that the model spans the correct values in a gross way. A detailed statistical comparison of the two time series is provided in section 4.

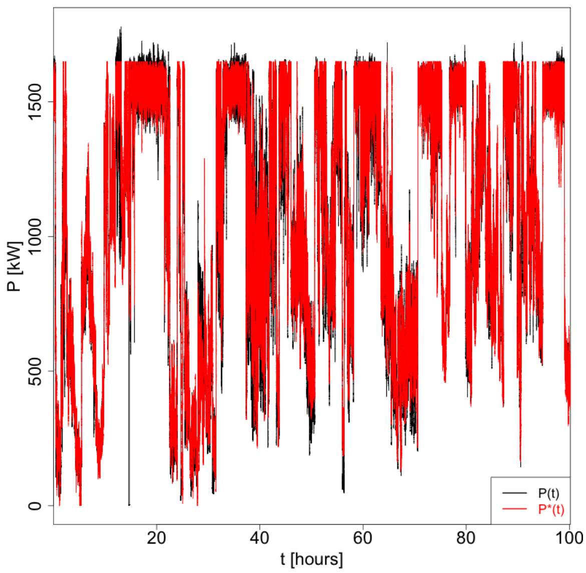

Figure 3: Comparison of $P(t)$ (black) and $P^{\star}(t)$ (red) for 100 hours at sampling frequency $2.5Hz$.

4 Statistical validation of the model

4.1 Ten-minute statistics

The time series displayed in figure 3 are visually similar, but this is not sufficient to validate the stochastic model. A statistical comparison of the measured and modeled time series $P(t)$ and $P^{\star}(t)$ is detailed in this section. One can decompose the series $P(t)$ into

$$P(t) = \langle P \rangle_{10min} + P_{remain}(t)\,, \qquad (4)$$

and similarly for $P^{\star}(t)$. $\langle P \rangle_{10min}$ represents the ten-minute average of $P(t)$, and $P_{remain}(t)$ gives the remaining fluctuations around the ten-minute average. While $\langle P \rangle_{10min}$ gives the slow ten-minute trend, $P_{remain}(t)$ represents the fast fluctuations resulting from turbulence.
Two comparisons are performed:

- the ten-minute average $\langle P \rangle$ characterizes the evolution on a long time scale (10 minutes). While this paper focuses more directly on faster fluctuations, it is important to reproduce the ten-minute evolution. The ratio $\langle P^{\star} \rangle_{10min}/\langle P \rangle_{10min}$ quantifies the quality of the model to reproduce the power production on the long time scale of 10 minutes;

- the ten-minute standard deviation $sd(P)_{10min}$ characterizes the magnitude of the remaining fluctuations[5]. The ratio $sd(P^{\star})_{10min}/sd(P)_{10min}$ quantifies the quality of the model to reproduce the fast, turbulent fluctuations in terms of magnitude.

Figure 4 illustrates visually the ability of the stochastic model to reproduce the power output time series on shorter time periods. The model manages to reproduce the power production of the WEC on both the slow trend, and also on the additional fluctuations. One can see in figure 4(b) that every ten minutes, the average and standard deviation of the two series are similar. Once the model was executed, and the entire time series of $P^{\star}(t)$ was generated, one can calculate all the ten-minute ratios of averages and standard deviations. The total ratio is defined as the average of all the ten-minute ratios. It is calculated for both the average and the standard deviation. The final ratios obtained are displayed in table 4.1.

[4] An optimal initial value is $P^{\star}(t=0) = P_{IEC}(\,u(t=0)\,)$, where $P_{IEC}(u)$ is the IEC power curve of the WEC.

[5] The standard deviation denoted $sd(P)_{10min}$ in this paper is calculated following $sd(P)_{10min} = \langle (P - \langle P \rangle_{10min})^2 \rangle_{10min}$.

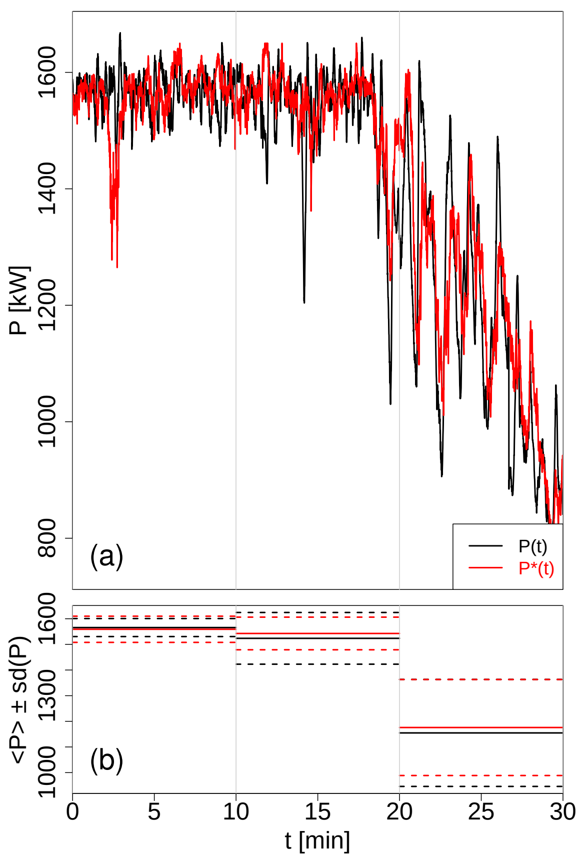

Figure 4: (a) Time series of $P(t)$ (black) and $P^\star(t)$ (red) for 30 minutes. (b) Ten-minute averages (full lines) and $\pm$ ten-minute standard deviations (dashed lines) with corresponding colors.

Table 1: Total ratio of ten-minute averages and of ten-minute standard deviations.

total $\frac{\langle P^\star \rangle_{10min}}{\langle P \rangle_{10min}}$	total $\frac{sd(P^\star)_{10min}}{sd(P)_{10min}}$
1.061	1.005

In the example presented, the ten-minute average of power is over-estimated by 6.1%, and the ten-minute standard deviation of power is over-estimated by 0.5%. These values can vary slightly, due to the randomness of the model. It should be noted that an optimization loop was applied to reach this result. The original ratio of standard deviations was in the order of 1.25 (over-estimation by 25%), due to natural deviations in the estimation of $D^{(2)}$, which is typically over-estimated[6]. $D^{(2)}$ was reduced in small steps until the total ratios presented in table 4.1 reached the desired value. The final value of $D^{(2)}$ is retained as the correct value for the model. As the ten-minute mean value is over-estimated by 6.1%, the optimization technique should be further improved.

4.2 Two-point statistics

All statistical quantities presented above are *one-point* statistics [16]. *Two-point* statistics such as the power spectral density (more commonly called *spectrum*) $S(f)$ are calculated following [17] for the two time series and compared in figure 5.

The overall shape of the spectrum is reproduced by the stochastic model. The most striking deviation is observed at frequency $f \approx 1Hz$, which corresponds to a $1Hz$ oscillation in the measured time series $P(t)$. While it seems possible that the peak observed here may be caused by the blades passing the tower of the WEC, no clear evidence was possible within the present study. This oscillation is not reproduced by the model,

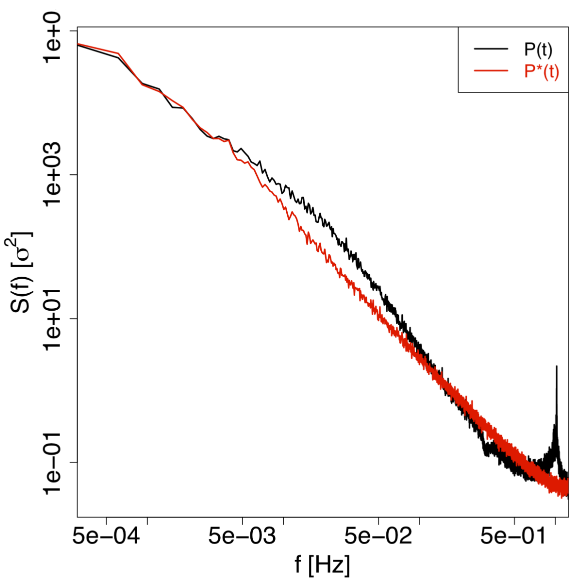

Figure 5: Power spectral density $S(f)$ of P (black) and $P^\star$ (red). $S(f)$ is normalized by the variance σ^2 of the time series.

[6] Such deviations are expected [15] as equation (2) applies in theory on continuous processes. However, the time series used in section 2 are imperfect due to measurement noise and to a finite sampling rate. A continuous process cannot be measured physically, and remains a purely mathematical object, making the optimization procedure necessary in many cases.

but could possibly be added to the model as a succeeding step.

An additional *two-point* quantity is the power increment $P_\tau(t) = P(t+\tau) - P(t)$, where τ is a given time scale. P_τ represents the change in power over a given time scale τ. When plotting the probability density function (PDF) $p(P_\tau)$ of the power increment P_τ, one can quantify the occurrence of gusts on the given time scale τ [16]. The increment PDF is given for various scales in figure 6.

Figure 6 illustrates the ability of the model

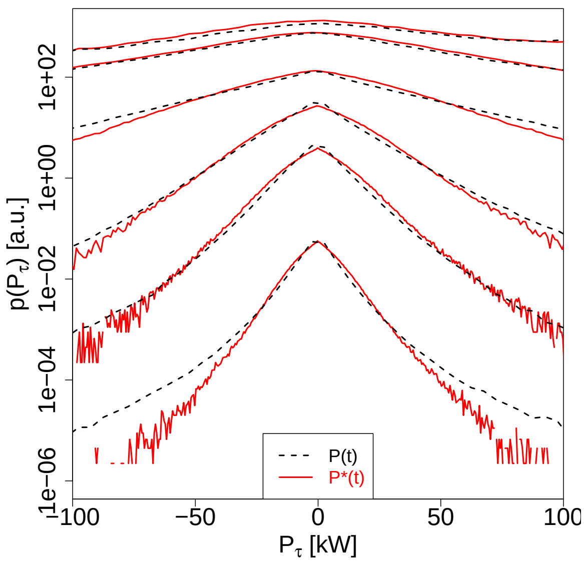

Figure 6: PDF $p(P_\tau)$ of power increments P_τ for various scales $\tau = (0.4, 0.8, 1.6, 6.4, 25.6, 26214.4)s$ (bottom to top curves shifted upwards for clarity). The red full lines are estimated from $P^\star$ and the black dashed lines from P. The *y-axis* is represented using a logarithmic scale.

to generate intermittent power gusts. For example, changes in power production up to $+100kW$ and $-100kW$ within $0.8s$ occur, as their probability is more than zero. This aspect is especially important on shorter time scales (represented by the lowest curves in figure 6) when fast wind gusts are converted into fast power gusts. The model does not create as many gusts on the shortest time scale (lowest curve) as deviations between the two curves can be seen. Improvements could be performed in this direction. Overall, the stochastic model still displays a valuable result as power gusts are mostly well reproduced, but maybe not often enough for the very fast ones on the shortest time scale. All results presented in figures 3 to 6 show a good agreement between the measured time series and the result of the stochastic model. For such, it is concluded that the stochastic model reproduces the intended statistics.

5 Conclusion

A stochastic model is introduced for the power production of a WEC. This model can generate a high-frequency time series of power output from a high-frequency time series of wind speed. In a first step, the dynamics of the particular WEC are brought into the model from an initial measurement of wind speed and simultaneous power output. From this calculation in section 2.2, the drift field $D^{(1)}$ gives a visual representation of the WEC dynamics at high frequency. The conversion from wind speed to power output appears as the superposition of an attractive power curve plus some additional fluctuations due to turbulence. The WEC would tend towards the power curve if the wind inflow were laminar, but the turbulent fluctuations always push the dynamics away from the power curve. While the drift field $D^{(1)}$ represents this attractive power curve, the diffusion field $D^{(2)}$ quantifies additional random fluctuations due to turbulence.

In a second step, the stochastic Langevin equation is solved using the two fields previously estimated. It is solved here using the wind speed time series used to estimate the fields, such that a direct comparison between the measured and modeled power time series is possible. While a first validation of the model can be done comparing visually the time series, a statistical comparison is performed in section 4. As a result of this test, the stochastic model reproduces the ten-minute average values of power with deviations of order $\approx 6\%$. This should be further improved through a more advanced optimization technique. The ten-minute standard deviations of power deviate from the measurement by less than 1%. This result is obtained using an optimization loop, that could be run further to reach even better correspondence. These results confirm the visual *similarity* of the two time series.

Additionally, two-point statistics are investigated. The spectrum of the power output time series is estimated. The spectrum of the modeled series displays a qualitative agreement with the measurement series, although a peak at $\approx 1Hz$ is omitted. This peak is attributed to the shadow effect of the tower on the rotating blades, and could possibly be inserted manually into the model. The PDF of power increments are also investigated. Satisfying results are obtained on a large range of time scales, indicating that the model reproduces the power *gusts* observed on measurements. The *turbulent* structures observed on power output measurements are reproduced qualitatively well.

Due to its simple structure, such model can be run fast on any conventional computer. The entire computation for 4 days of data at $2.5Hz$ was performed within 20 minutes on a desktop machine, using the interpreting language R. An implementation to a compiling language would greatly reduce the computation time, making the model even more flexible. This fast and flexible structure makes a power prediction model on the scale of wind farms (or larger) possible. One would need however a high-frequency measurement of wind speed to feed the model. Current research aims towards a similar model that could perform without high-frequency time series of wind speed, but simply using ten-minute average wind speed and turbulence intensity. A fast modeling of power production, power fluctuations and power "gusts" could then be performed for any WEC in any location based on only a wind speed measurement, or meteo model. A similar model for mechanical loads is also under development.

Acknowledgements

Parts of this work have been financially supported by the German Environment Ministry under grant number 0327642A, and by the German Ministry for Education and Research under grant number 0329372A. We would like to thank Stephan Barth, Julia Gottschall, Edgar Anahua and Michael Hölling for their pioneering work on stochastic analysis in wind energy applications.

References

[1] Böttcher, F., Barth, S., and Peinke, J., “Small and large scale fluctuations in atmospheric wind speeds,” *Stochastic Environmental Research and Risk Assessment (SERRA)*, Vol. 21, 2007, pp. 299–308.

[2] IEC, “Wind Turbine Generator Systems, Part 12: Wind turbine power performance testing,” International Standard 61400-12-1, International Electrotechnical Commission, 2005.

[3] Wächter, M., Gottschall, J., Rettenmeier, A., and Peinke, J., “Power curve estimation using LIDAR measurements,” *EWEC 2009 Proceedings*, 2009.

[4] Günther, H. and Hennemuth, B., *Erste Aufbereitung von flächenhaften Windmessdaten in Höhen bis 150 m*, Deutscher Wetter Dienst, BMBF-Projekt 0329372A, 1998.

[5] Körber, F., Besel, G., and Reinhold, H., *Meßprogramm an der 3MW-Windkraftanlage GROWIAN: Förderkennzeichen 03E-4512-A*, Große Windenergieanlage Bau- u. Betriebsgesellschaft, Hamburg, 1988, Bundesministerium für Forschung und Technologie.

[6] Jonkman, J., “NWTC Design Code FAST,” Tech. Rep. NREL/EL-500-38230, National Renewable Energy Laboratory, Golden, Colorado, USA, 2005.

[7] Milan, P., Mücke, T., Wächter, M., and Peinke, J., “Two numerical modeling approaches for wind energy converters,” *Proceedings of Computational Wind Engineering 2010*, 2010.

[8] Risken, H., *The Fokker-Planck equation*, 2nd ed., Springer, Berlin, 1989.

[9] Anahua, E., Barth, S., and Peinke, J., “Markovian power curves for wind turbines,” *Wind Energy*, Vol. 11, No. 3, 2008, pp. 219–232.

[10] Milan, P., Mücke, T., Morales, A., Wächter, M., and Peinke, J., "Applications of the Langevin power curves," *EWEC 2010 Proceedings*, 2010.

[11] Gottschall, J. and Peinke, J., "How to improve the estimation of power curves for wind turbines," *Environmental Research Letters*, Vol. 3, No. 1, 2008, pp. 015005 (7pp).

[12] Schneemann, J., Milan, P., Luhur, M. R., Knebel, P., and Peinke, J., "Lift measurements in turbulent flow conditions," *DEWEK 2010 conference proceedings*, 2010.

[13] Friedrich, R. and Peinke, J., "Description of a Turbulent Cascade by a Fokker-Planck Equation," *Physical Review Letters*, Vol. 78, No. 5, 1997, pp. 863–866.

[14] R Development Core Team, "R: A Language and Environment for Statistical Computing," 2010, ISBN 3-900051-07-0.

[15] Gottschall, J., *Modelling the variability of complex systms by means of Langevin processes*, Ph.D. thesis, Carl von Ossietzky Universität Oldenburg, Germany, 2009.

[16] Morales, A., Wächter, M., and Peinke, J., "Advanced Characterization of Wind Turbulence by Higher Order Statistics," *EWEC Proceedings 2010*, 2010.

[17] Press, W. H., Teukolsky, S. A., Vetterling, W. T., and Flannery, B. P., *Numerical recipes in C*, Cambridge University Press, 2nd ed., 1992.